

# Real-space renormalization-group approach to field evolution equations

Andreas Degenhard\*

*The Institute of Cancer Research, Department of Physics, Downs Road, Sutton, Surrey SM2 5PT, United Kingdom*

Javier Rodríguez-Laguna†

*Instituto de Matemáticas y Física Fundamental, CSIC C/Serrano 123, Madrid 28006, Spain*

(Received 21 June 2001; revised manuscript received 3 October 2001; published 12 February 2002)

An operator formalism for the reduction of degrees of freedom in the evolution of discrete partial differential equations (PDE) via real-space renormalization group is introduced, in which cell overlapping is the key concept. Applications to (1+1)-dimensional PDEs are presented for linear and quadratic equations that are first order in time.

DOI: 10.1103/PhysRevE.65.036703

PACS number(s): 02.60.Cb, 02.30.Jr, 64.60.Ak, 05.10.Cc

## I. INTRODUCTION

The use of real-space renormalization group (RSRG) techniques [1,2] to analyze questions related to the discretization of classical evolution field equations has recently raised a great deal of attention. Promising results have been achieved from the concept of *perfect action* [3] and its application to deterministic partial differential equations (PDE) [4,5]. Recently, the group of Hou, Goldenfeld, and McKane extended the idea to stochastic PDE [6] by using a space-time Monte Carlo formalism for classical problems [7]. In this last work, interesting nonlocal effects were discovered.

The present work tries to develop further the line traced in Ref. [5] generalizing the notion of *coarse graining*. The fields are assumed to be defined on spatial cells and a mechanism to define truncation operators is provided based on the *overlapping* of cells in different partitions of space. Both linear and nonlinear (1+1)-PDE are analyzed. Stochastic equations are not dealt with in the present work, but it should be noticed that the formalism of Ref. [6] may be easily adapted to include the new truncation operators.

This paper is organized as follows: Sec. II discusses the RSRG operator formalism that shall be applied. Our geometric construction of the truncation operators is explained in detail in Sec. III. Section IV is devoted to the exposition of some numerical results. Some concluding remarks and proposals for later work are discussed in the Sec. V.

## II. THE FORMALISM

Let  $\mathcal{P}$  be a partition of a given region of a manifold  $\mathcal{M}$ , composed of the cells  $\{C_i\}_{i=1}^N$ . Let  $\phi$  be a scalar field on that region of space and consider the discretization [8] associated to the partition

$$\phi_i \equiv \int_{\mathcal{M}} d\mu \phi(x), \quad (1)$$

where  $\mu$  is any measure on  $\mathcal{M}$ . Let us, furthermore, consider the following evolution equation, which we will assume exact [9]:

$$\partial_t \phi_i = H_{ij} \phi_j. \quad (2)$$

This scheme can hold easily any linear evolution equation, with a great variety of boundary conditions. Equation (2) may result from the discretization of any linear PDE (or even a nonlocal equation) within any explicit or implicit algorithm. The operator  $H$  shall be termed the *evolution generator*.

Some nonlinear equations may enter easily this formalism. For example, any quadratic evolution generator might be added as

$$\partial_t \phi_i = Q_{ijk} \phi_j \phi_k + H_{ij} \phi_j. \quad (3)$$

This allows study of surface growth phenomena as governed by the Kardar-Parisi-Zhang (KPZ) equation [10] or the related one-dimensional (1D) turbulence described by Burgers equation. More complex equations such as Navier-Stokes are by the moment out of reach of the formalism because the fields under study are not scalar.

The field discretizations as defined by Eq. (1) find their natural place in a vector space  $E^N$ . A truncation operator  $R: E^N \rightarrow E^M$  defines a subdiscretization within the original vector space. The effective field component indices shall be denoted with capital letters:  $\{\phi'_I\} \in E^M$ . The new discretization only provides  $M$  degrees of freedom and, thus, the  $R$  operator must have a nontrivial kernel.

The truncation operator shall be chosen to be linear [11]. This enables us to write its action as

$$\phi'_I = R_{Ii} \phi_i. \quad (4)$$

Had the  $R$  operator got a trivial kernel, an inverse operator  $R^{-1}$  might be written, which would be called the *embedding* operator. In this case the following equation would be exact:

$$\partial_t \phi'_I = H_{ij} R_{jI}^{-1} \phi'_J. \quad (5)$$

One might, therefore, evolve the effective discretization with only  $M$  degrees of freedom through equation,

\*Electronic address: andreasd@icr.ac.uk

†Electronic address: javirl@sisifo.imaff.csic.es

$$\partial_t \phi'_I = R_{II} H_{ij} R_{jJ}^{-1} \phi'_J \equiv H'_{IJ} \phi'_J, \quad (6)$$

where  $H'$  is the *renormalized evolution generator*. After the evolution of the reduced discretization has been completed, the evolution of the original discretization would be found

$$\phi_i(t) = R_{iI}^{-1} \phi'_I(t). \quad (7)$$

Equation (6) requires less storage and CPU time than Eq. (2) to be simulated on a computer. We may express this situation by the commutative diagram

$$\begin{array}{ccc} E^N & \xrightarrow{H} & E^N \\ R \downarrow & & \downarrow R \\ E^M & \xrightarrow{H'} & E^M \\ & & \uparrow R^{-1} \\ & & R \end{array}$$

Unfortunately, the situation displayed in the previous paragraph is impossible: the truncation operator must have a nontrivial kernel. Thus, it lacks a true inverse. Anyway, a “best possible” pseudoinverse may be found: an operator  $R^p$  that fulfills the Moore-Penrose conditions [12],

$$\begin{aligned} RR^pR &= R, & R^pRR^p &= R^p, \\ (R^pR)^\dagger &= R^pR, & (RR^p)^\dagger &= RR^p. \end{aligned} \quad (8)$$

These equations are solved only if  $R^p$  is the singular values decomposition (SVD) pseudoinverse of  $R$ .  $R^p$  is an “extrapolation” operator, which takes an  $E^M$  (reduced) discretization and returns an approximate  $E^N$  (full) one. The only important piece of information contained in  $R$  is its kernel, which represents the degrees of freedom that are removed (see, e.g., [13]).  $RR^p$  is the identity operator on  $E^M$  and  $R^pR$  is a projector on the *relevant degrees of freedom* subspace of  $E^N$ . These degrees of freedom are stored as the column of the matrix  $R$ . It is highly recommended to orthonormalize these column vectors, because  $R^p$  becomes simply  $R^\dagger$ .

Using the pseudoinverse  $R^p$  instead of  $R^{-1}$  the diagram above does not commute. The “*curvature*” represents the error of the procedure. The renormalized evolution generator is written as

$$H'_{IJ} = R_{II} H_{ij} R_{jJ}^p, \quad (9)$$

where indices are kept for clarity. A quadratic evolution generator would be transformed in this way,

$$Q'_{IJK} = R_{II} Q_{ijk} R_{jJ}^p R_{kK}^p. \quad (10)$$

This expression shall be shorthand as  $Q' = RQR^p$ . Higher degree operators are possible, of course.

The election of the  $R$  operator is the key problem. Ideally it should depend on the problem at hand, i.e., on the field equation and the observables we want to measure. In this paper a geometrical approach is introduced that is independent of the physics of the dynamical system, but uses a quasi-static truncation procedure for a careful selection of the relevant degrees of freedom.

The schedule for all the simulations that shall be presented in the rest of this work is as follows: (1) present a Hamiltonian  $H$  (at most quadratic) and an initial field  $\phi(0)$ ; (2) perform the exact evolution and obtain  $\phi(t)$ ; (3) propose a truncation operator  $R$  and obtain the pseudoinverse  $R^p$ ; (4) calculate the renormalized Hamiltonian and the truncated initial field:  $H' = RHR^p$  and  $\phi'(0) = R\phi(0)$ ; (5) perform the renormalized evolution on  $\phi'(0)$  and obtain  $\phi'(t)$ ; (6) compare  $\phi(t)$  and  $R^p\phi'(t)$ .

We distinguish between a *real-space error*, which is given by the  $L^2$  norm of  $[\phi(t) - R^p\phi'(t)]$  (a vector from  $E^N$ ) and the *renormalized space error*, which is given by the  $L^2$  norm of  $[R\phi(t) - \phi'(t)]$  (a vector from  $E^M$ ). Both errors need not be equal. It is impossible for the first error to vanish for all  $\phi(0)$  and all time, although that is possible for the second one. In that case, the retained degrees of freedom are *exactly evolved* after the rest of the information has been removed. Such a situation corresponds to a *perfect action*.

### III. GEOMETRIC TRUNCATION OPERATORS

In this section a set of construction rules for the  $R$  operator shall be presented that shall allow for practical computations.

Let us consider the 1D interval  $[0,1]$  and let  $\mathcal{P}_n$  denote a regular partition of that interval into  $n$  equal cells, denoted by  $C_i^m \equiv [(i-1)/n, i/n]$ . The truncation operator  $R^{M \leftarrow N}$  shall be defined by

$$R_{ii}^{M \leftarrow N} \equiv \frac{\mu(C_I^M \cap C_i^N)}{\mu(C_I^M)}, \quad (11)$$

where  $\mu(\cdot)$  denotes the standard measure in  $\mathbb{R}$ ,  $C_i$  is a cell of the source partition  $\mathcal{P}_N$ , and  $C_I$  is part of the destination one  $\mathcal{P}_M$ . In geometrical terms, the  $R$  matrix elements are given by the ratio

$$R_{ii}^{M \leftarrow N} = \frac{\text{Overlap between cells } C_i \text{ and } C_I}{\text{Measure of cell } C_I}. \quad (12)$$

The rationale behind this expression may be expressed with a physical analogy. Let us consider  $\phi_i$  as the density of a gas in the  $i$ th cell of the source partition, limited by impenetrable walls. Now a new set of walls is settled: the ones corresponding to the new (destination) partition. The old walls are, after that, removed. The gas molecules redistribute uniformly in each new cell. The new densities are the values  $\phi_I$  that constitute the transformed field discretization. Figure 1 should be helpful.

In more mathematical terms, the value of  $\phi_I$  is a linear estimate for

$$\phi_I = \int_{C_I} \phi(x) dx \quad (13)$$

conserving the total mass:  $\sum_I \phi_I = \sum_i \phi_i$ . Equation (11) may also remind of the definition for conditional probability.

The resulting  $R^{M \leftarrow N}$  operators shall be termed *sudden truncation operators*. Compared to standard RSRG integer

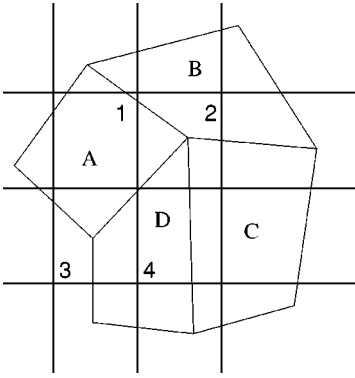


FIG. 1. A part of two overlapping partitions is depicted. The lines delimiting the “old” partition are thin (cells  $A, B, \dots$ ), while the thick lines belong to the “new” one (1, 2,  $\dots$ ). For example, there shall be no  $R$  matrix element between cells 1 and  $C$ , since they do not overlap. On the other hand, the matrix element  $R_{1A}$  must be close to 1.

factor blocking techniques [5], the operators  $R^{M \leftarrow N}$  allow for a greater flexibility. For example, it is possible to remove a *single degree of freedom* (see Fig. 2 for a 1D example). The sudden truncation operators do not form a closed algebra. The composition of sudden truncation operators shall take us to the concept of *quasistatic* or *adiabatic* truncation operators. These are defined by

$$qR^{M \leftarrow N} = R^{M \leftarrow M+1} R^{M+1 \leftarrow M+2} \dots R^{N-1 \leftarrow N}. \quad (14)$$

Of course,  $qR^{M \leftarrow N}$  differs greatly from  $R^{M \leftarrow N}$ . The term “quasistatic” is suggested by the thermodynamical analogy introduced before. The relation between quasistaticity and reversibility leads us to think that the  $qR^{M \leftarrow N}$  may be better suited to our purposes.

A single step sudden transformation is given analytically by

$$R_{ii}^{N-1 \leftarrow N} = \delta_{i,i} \frac{N-I}{N} + \delta_{i,i-1} \frac{I}{N}. \quad (15)$$

Iterating this relation it can be proved that the quasistatic operators fulfill the recursion relation,

$$qR_{ii}^{M \leftarrow N} = \frac{M+1-I}{M+1} qR_{ii}^{M+1 \leftarrow N} + \frac{I}{M+1} qR_{i+1,i}^{M+1 \leftarrow N}. \quad (16)$$

This relation allows to calculate the matrices using no matrix products. This expression improves greatly the efficiency of the numerical applications.

The degrees of freedom that are retained by the quasistatic truncation matrix are plotted in Fig. 3. They are the  $E^N$

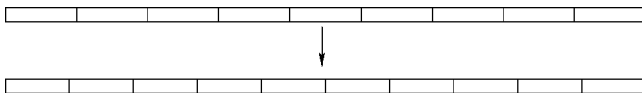


FIG. 2. The lower partition has just a single degree of freedom less than the one above. A truncation matrix may be written to proceed from one to the other.

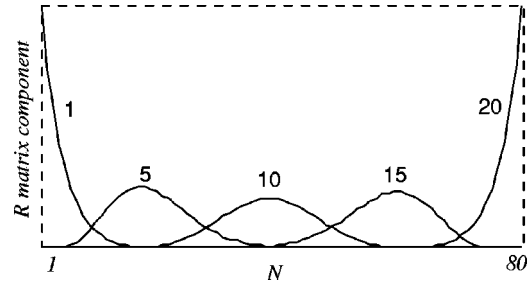


FIG. 3. Some of the degrees of freedom that are retained by the quasistatic truncation operator proceeding from  $80 \rightarrow 20$  sites. Cells 1, 5, 10, 15, and 20 are depicted. Notice that the “cells” are now overlapping and have slightly Gaussian nature.

vectors given by the columns of  $qR^{M \leftarrow N}$ .

Each of the discrete functions depicted in Fig. 3 may be considered to represent a relevant degree of freedom when truncating with the matrix  $qR^{20 \leftarrow 80}$ . Although the functions representing the degrees of freedom are now overlapping, they conserve a true real-space nature. It should be noticed that the width of the leftmost and rightmost cells is smaller than the one at the middle of the interval. A consequence is the quite exact representation of the boundary conditions.

It should be remarked that other authors have already introduced overlapping blocks within RSRG applications [14]. Intercell correlations, which are the key to the most successful RSRG algorithms [15,16], are usually captured more easily within an overlapping cells approach.

The most usual subdiscretization approach is the decimation method, where one degree of freedom out of every  $f$  is considered relevant. This truncation scheme may not be represented within our formalism. The reason is that the implementation on the field discretization is given by the matrix

$$D_{ii} = \delta_{fI,i}. \quad (17)$$

But the  $R$  matrix (17) along with its SVD pseudoinverse yields a trivial dynamics, because the retained degrees of freedom are *not in contact*. A possible solution to conserve linearity, though losing the Moore-Penrose conditions (8).

A discrete Fourier Transform along with a cutoff might be a suitable linear truncation procedure, but we shall not leave the RSRG setting: our relevant degrees of freedom do have a local geometric meaning.

#### IV. APPLICATIONS AND NUMERICAL RESULTS

This section discusses some numerical applications, both to linear and nonlinear examples.

##### A. Heat equation

The heat equation is defined on any space by stating that the evolution operator is given by minus the Laplacian on such a space. It is known that the Laplacian operator may be sensibly defined on a great variety of spaces [17], including discrete spaces [18].

Our 1D interval shall always be  $[0,1]$ . As it is split into  $N$  cells, the cells width is always  $\Delta x = 1/N$ . The structure is

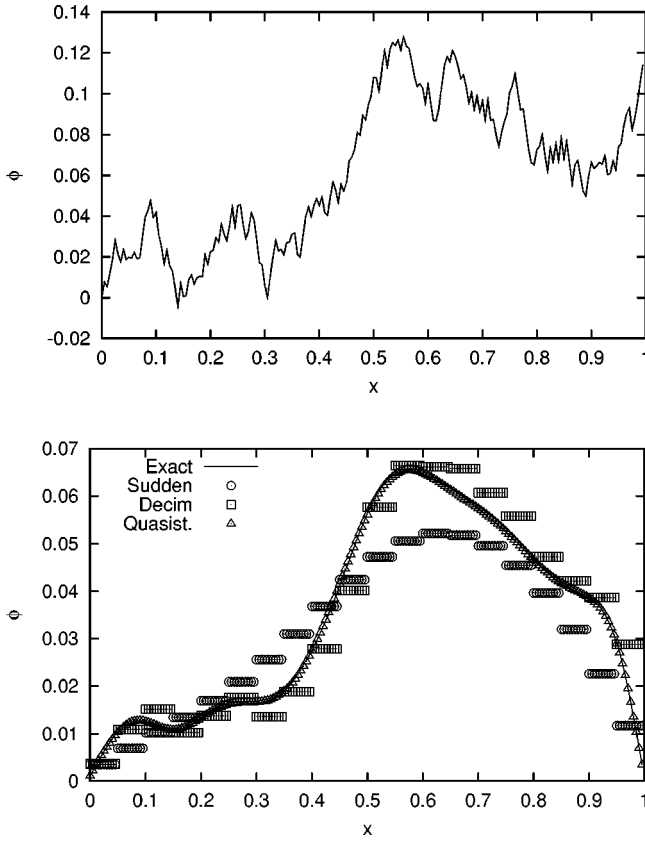


FIG. 4. A random increments function is taken as the initial condition (up) with 200 cells. Below, the continuous line shows the exact evolution under the heat equation with  $\kappa = \frac{1}{2}$ , along 500 time steps with  $\Delta t = 5 \times 10^{-6}$ . The triangles are given by the quasistatic approximation with 20 degrees of freedom. The circles represent the sudden approximation, and the squares follow the sudden approximation, i.e., conventional symmetric coarse graining.

given by the discrete Laplacian matrix on a linear graph,

$$L_{ij} = 2\delta_{i,j} - \delta_{|i-j|,1}, \quad (18)$$

with fixed boundary conditions  $L_{11} = L_{NN} = 2$ . The equation shall be given by

$$\partial_t \phi_i = -\frac{\kappa}{\Delta x^2} L_{ij} \phi_j. \quad (19)$$

The first test shall be a random increments initial condition, i.e., it fulfills the equation,

$$\phi_{i+1} = \phi_i + r, \quad (20)$$

with  $r$  a random variable with mean zero, equally distributed in an interval of width  $\Delta$ . Using  $N=200$ ,  $M=20$ , and  $\Delta = \frac{1}{4}$  (a quite severe reduction of a factor 10) we obtain the results depicted in Fig. 4. The errors for the results of Fig. 4 are summarized in Table I. Errors are noticed to be smaller in renormalized space. The reason is that in real space two sources of error get mixed: the possibility of representation of the initial data with the restricted degrees of freedom and

TABLE I. Comparative of errors between different truncation schemes for heat equation on the random-increments initial condition depicted in Fig. 4.

Method	Real-space error	Renormalized space error
Quasistatic	0.53%	0.29%
Sudden	20%	19%
Decimation	13%	4.7%

the dynamical relevance of the removed information. In renormalized space only the second type of error contributes.

To examine the relevant scaling laws [19], a discretization of  $\phi(x) = \delta(x - 1/2)$  is defined on the 200 cells partition, and is normalized according to

$$\sum_{i=1}^N \Delta x \phi_i = 1. \quad (21)$$

Under time evolution, the peak becomes a Gaussian function and its width  $W$  follows the law:

$$W(t) \equiv \sum_{i=1}^N i \Delta x \phi_i \sim t^{1/2}. \quad (22)$$

Equation (22) can be proved to be exact also in the discrete case as shown in the Appendix. Using the same constants as in the previous calculation, we have performed a quasistatic simulation of the same problem, and depicted in Fig. 5 a log-log plot of the width against time: The data from the quasistatic simulation in Fig. 5 fit, after a transient, to a straight line with slope  $0.4990 \pm 0.0001$ . The exact field evolution yields exactly the same value, without the transient. The sudden approximation saturates at long times. Usual decimation gives a correct result.

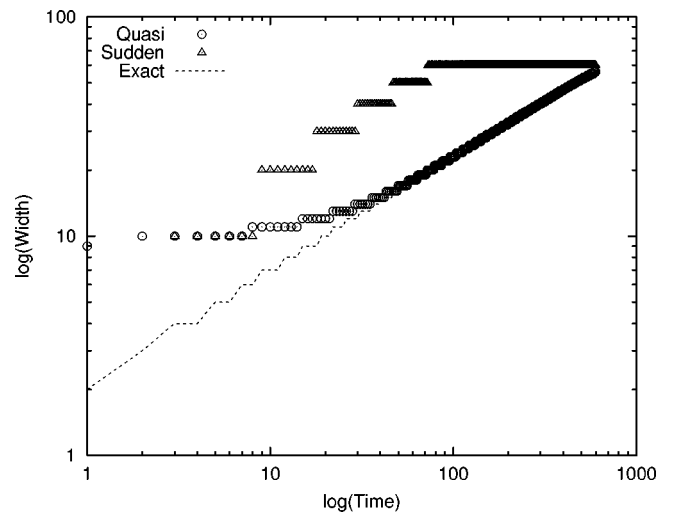


FIG. 5. Log-log plot of the width of the Gaussian against time. The steady straight line has slope  $\approx 0.5$ .

TABLE II. Low-energy spectrum of a particle in a box split into 100 discrete cells, calculated through exact diagonalization, and two effective variational RG techniques: sudden and quasistatic transformations.

Method					
Exact	0.000 967 435	0.003 868 8	0.008 701	0.015 460	0.024 13
Quasistatic	0.000 967 435	0.003 868 8	0.008 701	0.015 463	0.024 71
Sudden	0.008 101 410	0.031 749 3	0.069 027	0.116 917	0.171 53

### B. Low energy states in quantum mechanics

Researchers in RSRG methods have spent many efforts in developing techniques for the approximate obtention of the low-energy spectrum of quantum mechanical problems [13]. The reason was not the difficulty of the problem but of technical nature. With the development of the density matrix RG, correlated blocks RG, etc., [15,16] in the 90's, the problem was considered to be solved.

The quasistatic approach allows a very accurate approximation to the lowest energies of many quantum mechanical 1D systems. The transformation  $H \rightarrow H' = RHR^\dagger$  may yield an effective transformation of a Hamiltonian matrix, provided that the transformation  $R$  is orthogonal. In this case, the diagonalization of  $H'$  yields a *variational ansatz* approach to the real spectrum. The ansatz is of the form

$$|\Psi\rangle = \sum_{i=1}^M a_i |\phi_i\rangle, \quad (23)$$

where  $|\phi_i\rangle$  are the rows of  $qR^{M \leftarrow N}$  after an orthonormalization procedure, and the  $a_i$  are the variational parameters. The diagonalization of the quasistatically truncated Laplacian yields very precise values. For example, if  $N=100$  and  $M=10$ , we obtain the values for the spectrum of  $-L$  exposed in Table II.

The bad results for the sudden approximation are a bit misleading [20]. For example, the real-space error measured according to the  $L^2$  norm for the ground state is only around 11%. The source of error is the lost of smoothness. The rest of the eigenvalues (up to 10) do not fit as well as the first ones.

The method has also been tested with the harmonic oscillator and other potentials with equally good results, as long as the wave functions are smooth. In case of a potential given by  $V_i = V(x_i)$ , the Hamiltonian operator is just  $-L_{ij} + V_i \delta_{ij}$ .

### C. Kardar-Parisi-Zhang equation

The Kardar-Parisi-Zhang equation is widely used as a model of stochastic and deterministic surface growth [10]. Here we use the deterministic form defined as

$$\partial_t \phi = \lambda |\nabla \phi|^2 + \kappa \nabla^2 \phi \quad (24)$$

representing a surface in which absorption/desorption phenomena take place. The squared gradient term shall be implemented through the quadratic operator

$$K_{ijk} = \frac{1}{4} (\delta_{j,i+1} - \delta_{j,i-1}) (\delta_{k,i+1} - \delta_{k,i-1}), \quad (25)$$

which is obtained through the centered derivatives approximation to the gradient [21]. Boundary conditions are imposed for which forward and backward derivatives are employed. The first test evolves an initial condition given by a sinusoidal function  $\phi(x) = \sin(4\pi x)$  with  $x \in [0,1]$ . The resolution change is  $40 \rightarrow 20$  and 2000 time steps with  $\Delta t = 5 \times 10^{-6}$  were simulated. Figure 6 shows the results for  $\lambda = 2$  and  $\kappa = 1/2$ . The errors for such a test are given in Table III. A different test was carried out with a random increments function, as for the heat equation. The rest of the parameters are the same as in the previous simulation. The results of this simulation are displayed in Fig. 7 and the numerical errors are provided in Table IV.

Some more nonlinear equations have been tried, such as Burgers [22] and others, with comparable results. We encourage the reader to experiment.

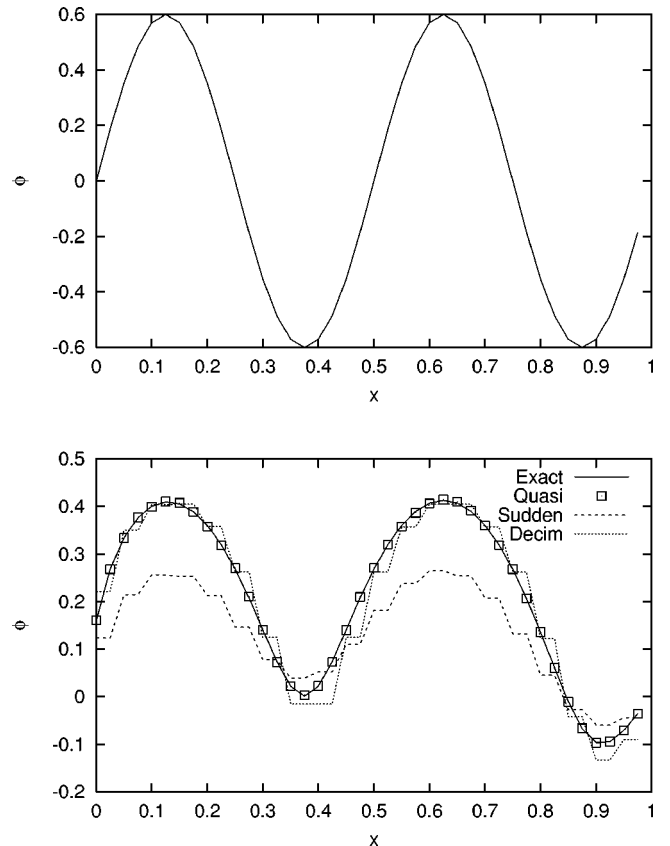


FIG. 6. A sinusoidal surface profile evolved by the KPZ dynamics with the parameters explicitly given in the text. Notice that a slight asymmetry in the initial function (a lattice artifact) develops a high asymmetry in the exact and quasistatic approximations.

TABLE III. Errors in the evolution of a sinusoidal initial condition under KPZ equation, corresponding to the results of Fig. 6. The parameters are explicitly given in the text.

Method	Real-space error	Renormalized space error
Quasistatic	0.5%	0.2%
Sudden	39%	38%
Decimation	15%	8%

#### D. Efficiency issues

A problem which must be remarked is that the approximation renders new evolution generators which may have a greater number of nonnull entries than the originals. The elements typically decrease in magnitude as a power of their distance to the diagonal, albeit they often alternate signs. This corresponds to the nonlocal space-time effects remarked by Hou, Goldenfeld, and McKane [6].

This fact forces the practitioner to make computational complexity estimates before trying this method. Various factors should be pondered:

(1) *Reduction factor attainable for a given equation.* KPZ stands more than 50% reduction for a wide set of initial conditions. The heat equations stands more than 90%.

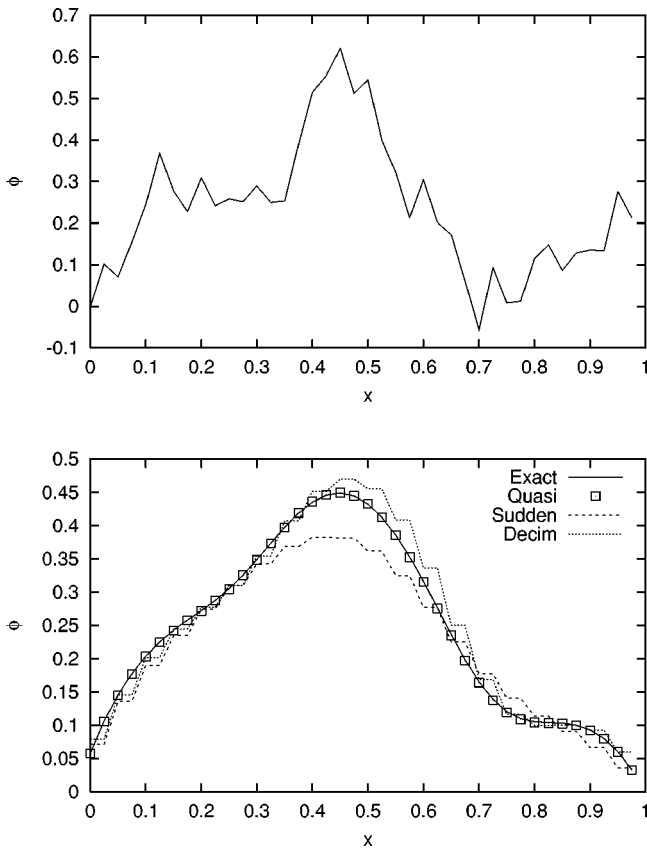


FIG. 7. Random increments function (above) built in the same way as that of Fig. 4. Below, the exact evolution is displayed by the continuous line. Squares mark the quasistatic truncation approximation, while the dashed lines follow the sudden and the decimation truncations.

TABLE IV. Errors corresponding to the field evolution of a random-increments initial condition, shown in Fig. 7.

Method	Real-space error	Renormalized space error
Quasistatic	0.23%	0.23%
Sudden	12%	11%
Decimation	9.4%	6.5%

(2) *Availability and stability of local explicit methods.* If implicit methods must be used, or the equation has nonlocal nature, then the original equation is already long ranged and no loss of efficiency comes from applying the RSRG recipe described.

#### V. CONCLUSIONS AND FUTURE PROSPECTIVES

A formalism has been provided to deal with the reduction of degrees of freedom for a wide set of field evolution equations. The basis of the formalism is the *integral* specification of the field values (i.e., it is related to finite volume methods). The key concept to find the transformation between a partition of space and another is the *overlapping* of cells.

Our specific recipe stands removal of 90% of the degrees of freedom without distortion for linear PDE such as the heat equation, and 50% reduction without appreciable loss of accuracy for KPZ and related nonlinearities.

The main handicap of the technique is shared by all known strategies to the reduction of degrees of freedom: the appearance of nonlocal effects that may spoil the efficiency [6]. Future works on this algorithm should try to find suitable short-ranged approximations to the renormalized evolution generators. Also the extension to stochastic PDE makes nonlocal effects appear: a spatially white noise shall develop a nontrivial covariance matrix. The eigenfunctions of this matrix would be the appropriate basis.

It is easy to generalize the formalism to higher dimensions, but the algorithms to find cell overlappings is trickier. Nevertheless, fields of vectorial nature do not fit well in this formalism. The authors are developing a “difference forms” theoretical frame to deal with them, in the line traced by Katz and Wiese [4].

But the main interest of the authors at the present moment is a different extension: to find an algorithm in which the degrees of freedom are not of geometric nature, but are *chosen* by the equation itself.

#### ACKNOWLEDGMENTS

The authors would like to thank R. Cuerno, M. A. Martín-Delgado, S. N. Santalla, and G. Sierra for very useful discussions.

#### APPENDIX: SCALING OF THE DISCRETE HEAT EQUATION

In this appendix the exactness of relation (22) subject to any coarse-graining procedure keeping the normalization condition (13) is proved.

We generalize the definition in Eq. (22) to the expectation value for any observable  $O$  on a one-dimensional lattice composed of  $N$  sites according to

$$\langle O \rangle_t = \sum_{i=1}^N O_{t,i} \Delta x \phi_{t,i} \quad (\text{A1})$$

with the total time  $t = n\Delta t$  and  $n$  the number of discrete time evolutions.

Relation (22) also describes Brownian motion on a 1D lattice. According to Wick's theorem [23], it is sufficient to prove the linear dependence of the second moment  $\langle x^2 \rangle$  on time for any discretization scale, as the following proposition states:

*Proposition.* The second moment  $\langle x^2 \rangle$  as defined by definition (22) for the diffusion field  $\phi$  is given by (supposing free or periodic boundary conditions)

$$\langle x^2 \rangle_t = 2\kappa t + C(\phi_{t=0}), \quad (\text{A2})$$

subject to the normalization constraint (21). Here,  $C(\phi_{t=0})$  is a constant that depends on the initial field configuration and, for a  $\delta$  initial condition,  $C(\phi_{t=0}) = 0$ . In Eq. (A2),  $t$  is the time,  $\kappa$  is the diffusion constant, and no dependence on the discretization scale  $\Delta x$  is involved.

Using definition (A1) to define the second moment  $\langle x^2 \rangle$  we have

$$\begin{aligned} \langle x^2 \rangle_{t+1} &= \sum_{i=1}^N \Delta x (i\Delta x)^2 \phi_{t+1,i} \\ &= \sum_{i=1}^N i^2 (\Delta x)^3 \left[ \frac{\Delta t \cdot \kappa}{(\Delta x)^2} (\phi_{t,i-1} - 2 \cdot \phi_{t,i} + \phi_{t,i+1}) \phi_{t,i} \right]. \end{aligned} \quad (\text{A3})$$

The evolution equation uses a discrete Laplacian (18) and a forward time Euler scheme [21]. Some algebra and index shifting, along with the supposition of either free or periodic boundary conditions lead to

$$\langle x^2 \rangle_{t+1} = 2\kappa \Delta t \sum_{i=1}^N \{\Delta x \phi_{t,i}\} + \langle x^2 \rangle_t. \quad (\text{A4})$$

The equation is rewritten, taking into account that Eq. (21) is valid for all time, as

$$\langle x^2 \rangle_{t+1} = 2\kappa \Delta t + \langle x^2 \rangle_t. \quad (\text{A5})$$

Iterating the procedure  $n$  times yields the final result,

$$\langle x^2 \rangle_{t+1} = 2\kappa(t+1) + \langle x^2 \rangle_{t=0}. \quad (\text{A6})$$

Defining  $C(\phi_{t=0}) \equiv \langle x^2 \rangle_{t=0}$  and changing the index  $t+1$  to  $t$  we get the result stated in the above proposition. If the initial field configuration  $\phi_{t=0}$  is provided by the  $\delta$  peak that was used to generate Fig. 5, Eq. (A6) simplifies to

$$\langle x^2 \rangle_t = 2\kappa t. \quad (\text{A7})$$

Equation (A7) is equivalent to the calculation of the mean squared distance of a random walker after the time  $t$  starting at the center position, i.e., the location of the  $\delta$  peak.

- 
- [1] L. P. Kadanoff, *Physics* (Long Island City, N.Y.) **2**, 263 (1966).  
 [2] N. Goldenfeld, *Lectures on Phase Transitions and the Renormalization Group* (Addison-Wesley, Reading, MA, 1993).  
 [3] P. Hasenfratz and F. Niedermayer, *Nucl. Phys. B* **414**, 785 (1994).  
 [4] E. Katz and U.-J. Wiese, *Phys. Rev. E* **58**, 5796 (1998); e-print comp-gas/0709001.  
 [5] N. Goldenfeld, A. McKane, and Q. Hou, *J. Stat. Phys.* **93**, 699 (1998); e-print cond-mat/9802103.  
 [6] Q. Hou, N. Goldenfeld, and A. McKane, *Phys. Rev. E* **63**, 36 125 (2001); e-print cond-mat/0009449.  
 [7] M. F. Zimmer, *Phys. Rev. Lett.* **75**, 1431 (1995).  
 [8] Maybe the word *discretization* is slightly misleading, since no sampling is assumed. Furthermore, integral values are required.  
 [9] The perfect actions project aims at the removal of lattice artifacts on the discretizations of a continuous system. This work shall assume the discrete equation to be correct, along with all its lattice-dependent results.  
 [10] M. Kardar, G. Parisi, and Y. C. Zhang, *Phys. Rev. Lett.* **56**, 889 (1986); A. L. Barabási, and H. E. Stanley, *Fractal Concepts in Surface Growth* (Cambridge University Press, Cambridge, 1995).  
 [11] Linearity on the truncation operator is a highly nontrivial imposition. It forces the nonmixing nature of evolution generators of different *arity*, i.e.: a purely quadratic PDE may not develop a linear term under such a RG construction. This is doubtful, e.g., for Navier-Stokes equation, where the nonlinear term is supposed to develop a contribution to the viscous (linear) term.  
 [12] G. H. Golub and C. F. van Loan, *Matrix Computations* (Hopkins University Press, Baltimore, MD, 1996).  
 [13] J. González, M. A. Martín-Delgado, G. Sierra, and A. H. Vozmediano, in *Quantum Electron Liquids and High- $T_c$  Superconductivity* (Springer, New York, 1995).  
 [14] A. Degenhard, *J. Phys. A* **33**, 6173 (2000); A. Degenhard, *Phys. Rev. B* **64**, 174408 (2001).  
 [15] S. R. White, *Phys. Rep.* **301**, 187 (1998), and references therein.  
 [16] M. A. Martín-Delgado, J. Rodríguez-Laguna, and G. Sierra, *Nucl. Phys. B* **473**, 685 (1996); e-print cond-mat/9512130.  
 [17] S. Rosenberg, *The Laplacian on a Riemannian Manifold* (Cambridge University Press, Cambridge, 1997).

- [18] B. Bollobás, *Modern Graph Theory* (Springer, New York, 1998).
- [19] G. I. Barenblatt, *Scaling, Self-Similarity and Intermediate Asymptotics* (Cambridge University Press, Cambridge, 1996).
- [20] For some problems a  $L^2$  norm is clearly insufficient. Two functions may be quite alike, and lead to rather different physics if, for example, one has a small amplitude but high frequency oscillation (*Zitterbewegung*) superimposed on it. A discrete Sobolev space would be the correct mathematical tool.
- [21] W. H. Press, S. A. Teukolsky, W. T. Vetterling, and B. P. Flannery, *Numerical Recipes in C* (Cambridge University Press, Cambridge, 1992).
- [22] Of course, Burgers is intimately related to KPZ, but this does not imply that an algorithm that suits well to one of them must suit also the other.
- [23] C. Itzykson and J.-M. Drouffe, *Statistical Field Theory* (Cambridge University Press, Cambridge, 1994).